Composites Part A 108 (2018) 89–98

Contents lists available at ScienceDirect

Composites Part A

journal homepage: www.elsevier.com/locate/compositesa

Preparation and properties of carbon nanotubes/carbon fiber/poly (ether ether ketone) multiscale composites

Yanan Su[a,b], Shouchun Zhang[a], Xinghua Zhang[a], Zhenbo Zhao[a], Deqi Jing[a,*]

[a] National Engineering Laboratory for Carbon Fiber Technology, Institute of Coal Chemistry, Chinese Academy of Sciences, Taiyuan 030001, China
[b] University of Chinese Academy of Sciences, Beijing 100049, China

ARTICLE INFO

Keywords:
A. Multifunctional composites
B. Mechanical properties
C. Electrical properties
D. Thermal properties

ABSTRACT

The carbon nanotubes/carbon fiber/poly (ether ether ketone) (CNTs/CF/PEEK) multiscale composites with excellent properties were prepared by introducing treated CNTs (t-CNTs) into CF/PEEK composites using prepreg spraying method. The effect of t-CNTs content on the mechanical performance of composites such as interlaminar shear strength (ILSS), flexural strength and flexural modulus were investigated. The results indicated that the ILSS, flexural strength and flexural modulus of CNTs/CF/PEEK composites were increased by 35.8%, 25.4% and 23.7% after 0.5 wt% t-CNTs introducing. The surface of prepregs and cross-section of the composites displayed evenly t-CNTs dispersion and strong fiber-resin adhesion by scanning electron microscope observation. With the addition of t-CNTs, the electrical conductivity and thermal conductivity of CNTs/CF/PEEK composites were also markedly improved, in comparison with that of CF/PEEK composites. This suggested that the prepreg spraying method was an effective approach to coat t-CNTs on CF/PEEK prepregs and enhance the performance of CNTs/CF/PEEK composites.

1. Introduction

Carbon fiber reinforced polymer composites (CFRPs) have been widely used in aerospace, automotive, marine over the past few decades, due to their low weight and superior mechanical properties [1–3]. To meet the rising demand in structural damage sensing, structural batteries and anti-lighting strike applications, CFRPs with specific types of enhanced functionality, such as electrical conductivity and thermal conductivity, are required [4,5]. However, the multifunctional use of CFRPs is frequently limited by poor interfacial properties, low electrical and thermal conductivity when they are used in above-mentioned application. To solve these problems, multiscale composites should be prepared by introducing nanofillers into CFRPs, which would further improve the mechanical, electrical and thermal properties of CFRPs [6–10].

Carbon nanotubes (CNTs) show high specific surface area and aspect ratio, combined with excellent mechanical, electrical and thermal properties, so they are promising candidate nanofillers for developing of multifunctional composites [11–14]. Generally, CNTs were incorporate into fiber reinforced polymer composites (FRPs) system by dispersing it into matrix [13,14], growing or grafting on the fibers surface [15,16] and inserting CNTs buckypaper on laminar interface [11]. These approaches could enhance multifunctional properties of composites, but most studies related to multiscale composites focus on thermosetting resin. The reports on thermoplastics composites are scarce, especially for high-performance thermoplastic composites. The reason may be thermoplastic composites with a highly viscous matrix, thus it is difficult to effectively manufacture CNTs-integrated thermoplastic laminates. For example, CNTs/glass fiber/PEEK composite was obtained through mixing CNTs and PEEK resin, where the prepared composite showed excellent ILSS, electrical conductivity and thermal conductivity [13]. CNTs/glass fiber/PA-6 composite was prepared by firstly mixing the CNTs and PA-6 resin [14]. The dispersion of CNTs within the matrix resin will leads to an increase of matrix viscosity, which is incompatible with manufacturing thermoplastic composites. Besides mixing CNTs with matrix resin, directly depositing CNTs on carbon fiber was another method to prepare CNTs-integrated thermoplastic laminates. CNTs/CF/PP composite was prepared by firstly coating CNTs on fiber surface using chemical vapor deposition (CVD) [15]. However, this method is complex and it is unfavorable for its large-scale manufacture. Because of the drawbacks of above-mentioned methods, it is urgent and important to find a facile approach for the preparation of CNTs-integrated thermoplastic composites.

As a high-performance thermoplastic composites, carbon fiber/poly (ether ether ketone) (CF/PEEK) composites exhibit a unique combination of superior mechanical properties, chemical and flame resistance,

* Corresponding author.
E-mail address: jingdq@sxicc.ac.cn (D. Jing).

https://doi.org/10.1016/j.compositesa.2018.02.030
Received 14 October 2017; Received in revised form 2 February 2018; Accepted 20 February 2018
Available online 21 February 2018
1359-835X/

Table 1
Basic characteristic of unidirectional CF/PEEK semi-prepreg.

Prepreg type	Resin content (wt%)	Density (g/cm^3)	Thickness (mm)	Width (mm)
CF/PEEK	30 ± 3	1.61 ± 0.02	0.125 ± 0.01	70 ± 0.5

hydrothermal and dimensional stability, cost-effective processing and recyclability [17–19]. Owing to its superior performance, CF/PEEK has been widely applied in electronics, oil-gas, marine and aerospace industries [20–22]. However, the stronger mechanical properties and multifunctional properties of CF/PEEK composites are needed to meet more demanding applications. In this work, to develop its structural and multifunctional applications, CNTs/CF/PEEK multiscale composites were prepared by directly spraying t-CNTs onto CF/PEEK prepregs, which is prepreg spraying method. The resultant prepregs plies were then stacked and consolidated by compression molding. It was illustrated that the prepreg spraying method was well compatible with the current continuous carbon fiber reinforced high-performance thermoplastic composites manufacturing process. Moreover, the effect of t-CNTs on the interlaminar shear strength (ILSS), flexural strength and flexural modulus as well as electrical conductivity and thermal conductivity of CNTs/CF/PEEK multiscale composites were also systematically investigated.

2. Experimental

2.1. Materials

The unidirectional CF/PEEK semi-prepregs used in this study were supplied by the Institute of Coal Chemistry, Chinese Academy of Sciences, and the basic characteristics are listed in Table 1. Toray T700S was selected to prepare CF/PEEK semi-prepregs. Multi-walled carbon nanotubes (MWCNT, diameter of 10–20 nm, length of 10–30 μm) were purchased from Boyu New Material Technology Co. Ltd. (China). Prior to using, CNTs were treated by a mixture of H_2SO_4 and HNO_3 (3:1 V/V) under ultrasonic treatment for 8 h to form the oxygen functional group on CNTs surfaces at room temperature, which would conducive to CNTs dispersion. Thereafter, the treated CNTs were washed by deionized water and vacuum-dried for use, and it was denoted as t-CNTs.

2.2. Preparation of CNTs/CF/PEEK multiscale composites

The preparation process of CNTs/CF/PEEK multiscale composites was depicted in Scheme 1. Firstly, the CF/PEEK prepregs were cut into 70 mm × 70 mm ply. The different content of t-CNTs (0.1 wt%, 0.3 wt %, 0.5 wt% and 1.0 wt%) were dispersed in deionized water under ultrasonic treatment. It should be noticed that the content of t-CNTs was calculated on the basis of weight ratio of CF/PEEK prepregs. Then the t-CNTs dispersion was sprayed onto the CF/PEEK prepregs by spray gun (with an exit diameter of 0.2 mm). In order to speed up the evaporation of water, the heating plate was used and the temperature was set as 120 °C. 16 plies of CF/PEEK prepregs with t-CNTs were stacked by handing lay-up. Finally, the CNTs/CF/PEEK composite panels were manufactured by compression molding at 400 °C for 1 h at 30 MPa. The composite panels were cut into specified samples by a diamond saw blade for characterization. For the sake of comparison, the CF/PEEK composites without t-CNTs were also prepared by aforementioned procedures.

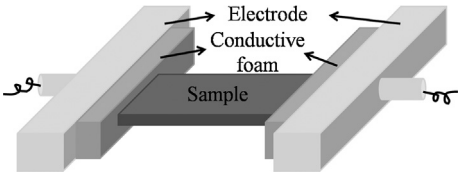

Scheme 2. Schematic of electrical conductivity test.

2.3. Characterization

2.3.1. X-ray photoelectron spectroscopy analysis

The surface chemical composition and functional groups on untreated CNTs (u-CNTs) and t-CNTs were characterized by X-ray photoelectron spectroscopy (AXIS ULTRA DLD, Japan) with an Al Kα X-ray source. The test thickness of sample is 1–3 nm and the results of sample were analyzed by XPSPeak software.

2.3.2. Morphology and dispersion state analysis

The morphology of t-CNTs on prepregs and the fracture surface of composites after mechanical test were characterized by a field emission scanning electron microscope (FE-SEM, JSM-7001F, Japan) at an accelerating voltage of 10 kV. The specimens were coated with Au-Pd alloy layer to avoid charge accumulation.

The dispersion state of t-CNTs on CF was characterized by energy dispersive spectroscopy (EDS) at an accelerating voltage of 15 kV.

2.3.3. Short-beam shear tests

Short-beam shear (SBS) tests were performed to determine the ILSS of CNTs/CF/PEEK composites according to ASTM D2344. It was conducted by a Universal Testing Machine (AG-10kN, Japan) with three-point bending (TPB) testing mode at a constant speed of 1.0 mm/min and a span-to-thickness ratio of 4. The ILSS values (τ_{ILSS}) were calculated using Eq. (1):

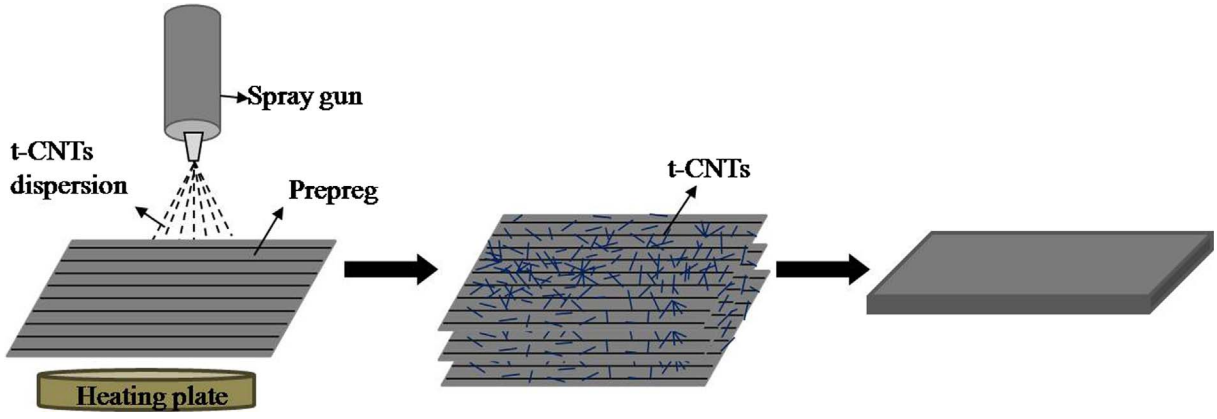

Scheme 1. The preparation process of CNTs/CF/PEEK composites. (For interpretation of the references to color in this figure legend, the reader is referred to the web version of this article.)

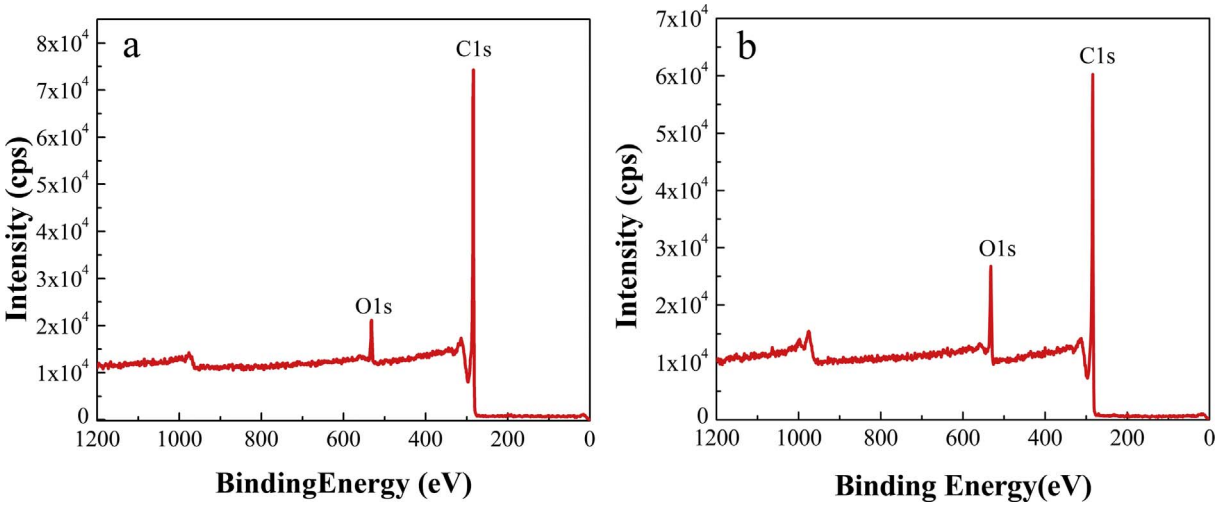

Fig. 1. The XPS wide-scan spectra of (a) u-CNTs and (b) t-CNTs. (For interpretation of the references to color in this figure legend, the reader is referred to the web version of this article.)

Table 2
Surface elemental composition of u-CNTs and t-CNTs (%).

	C1s		O1s		N1s		O/C
CNTs	BE/eV	AC/at.%	BE/eV	AC/at.%	BE/eV	AC/at.%	(%)
u-CNTs	284.45	94.29	532.55	5.25	400.20	0.46	5.57
t-CNTs	284.40	89.74	532.65	9.72	400.10	0.53	10.83

$$\tau_{ILSS} = 0.75\frac{P_m}{bh} \quad (1)$$

where b is the width of specimen and h is the thickness of specimen. The P_m was the maximum load during measuring. At least five samples were recorded for each specimen in above tests.

2.3.4. Flexural properties test

The 0° flexural tests of CF/PEEK and CNTs/CF/PEEK were also conducted by a Universal Testing Machine (AG-10kN, Japan) with TPB testing mode at a constant speed of 1.0 mm/min and a span-to-thickness ratio of 25 in accordance with ASTM D7264. The specimen width was 13 mm and the specimen length was at least 20% longer than the support span. The flexural strength (σ_f) and flexural modulus (E_f) were calculated using Eqs. (2) and (3):

$$\sigma_f = \frac{3P_m L}{2bh^2} \quad (2)$$

$$E_f = \frac{L^3 m}{4bh^3} \quad (3)$$

where L is the support span; b is the specimen width; h is the specimen thickness; P_m is the maximum load and m is the slop of the secant of the force-deflection curve. Also, at least five samples were recorded for each specimen in above tests.

2.3.5. Electrical conductivity measurements

Electrical conductivity (σ) was calculated using Eq. (4):

$$\sigma = \frac{1}{\rho} \quad (4)$$

And electrical resistivity (ρ) was calculated using Eq. (5):

$$\rho = R\frac{S}{L} \quad (5)$$

where R is the electrical resistance of composites. The S and L are the cross-sectional area and the length along the direction of materials resistance, respectively. R was measured in two directions (fiber axial directions and through-thickness) by DC low resistance tester (GF 2516A, China). In the test, conductive foam was used to eliminate contact resistance (R_{foam} < 80 mΩ). Before test, specimens were not polished based on the practical application of composites, thus the CF

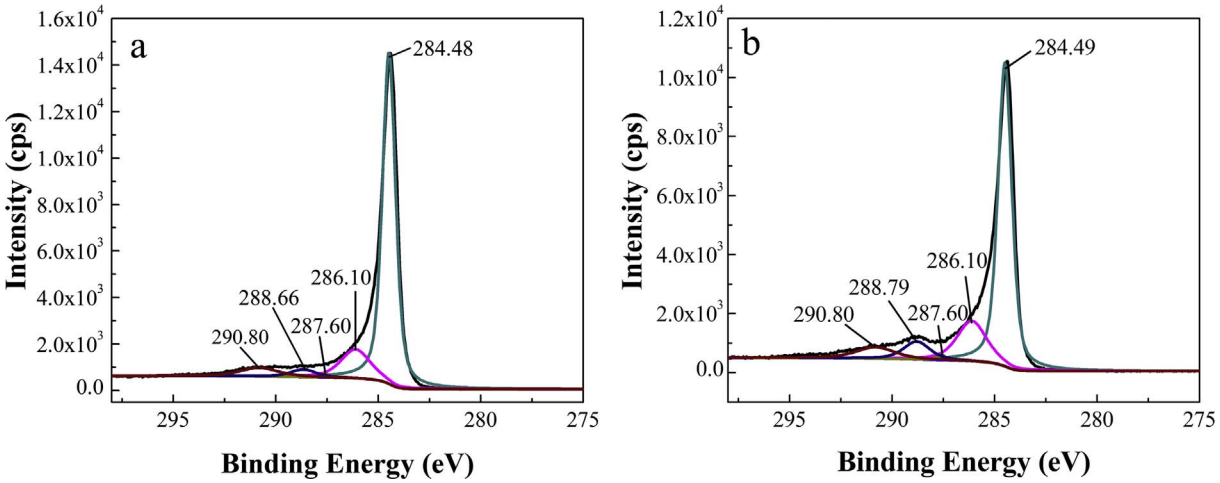

Fig. 2. C1s peak-fitting results: (a) u-CNTs and (b) t-CNTs. (For interpretation of the references to color in this figure legend, the reader is referred to the web version of this article.)

Table 3
Fitting results of C1s peaks (%).

CNTs		Peak assignment					
		Graphitic C	−C−OH −C−OR	−C=O	−COOH −COOR	π–π*	Oxygen-containing functional group (%)
u-CNTs	BE/eV	284.48	286.10	287.60	288.66	290.80	24.34
	PC/%	75.66	14.88	0.29	3.40	5.77	
t-CNTs	BE/eV	284.49	286.10	287.60	288.79	290.80	33.64
	PC/%	66.36	18.65	0.72	7.36	6.91	

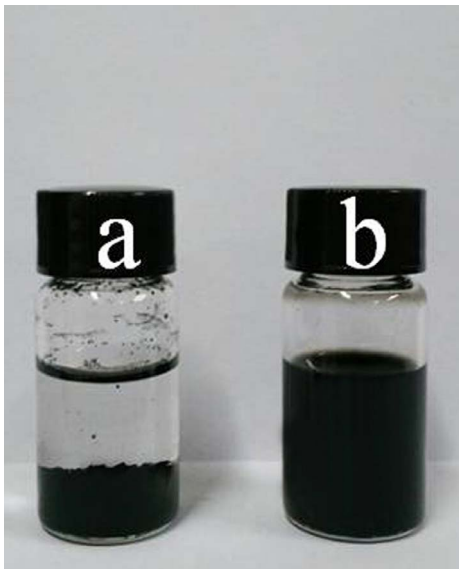

Fig. 3. The digital photos of CNTs dispersion: (a) u-CNTs (within 1 min) and (b) t-CNTs (after 10 months).

was not revealed. The schematic of electrical conductivity test was depicted in Scheme 2.

2.3.6. Thermal conductivity measurements

The thermal conductivity (κ) of composites was calculated using Eq. (6):

$$\kappa = \alpha C_p \rho \tag{6}$$

where thermal diffusion coefficient (α) was measured using a laser flash thermal analyzer (LFA 447/2-2lnsb NanoFlash). The specific heat (C_p) was measured by using a differential scanning calorimeter (DSC, 200 F3). The density (ρ) of composites was calculated using Eq. (7):

$$\rho = \frac{m}{V} \tag{7}$$

where m is the mass of composites and V is the volume of composites.

3. Results and discussion

3.1. The X-ray photoelectron spectroscopy of CNTs

XPS was used to characterize the elemental compositions of u-CNTs and t-CNTs surface. The wide-scan XPS spectra of CNTs are given in Fig. 1. The peaks at around 284.45 eV and 532.55 eV could be attributed to C1s and O1s, respectively. The binding energies (BE) of each peak and the corresponding atomic concentration (AC) of u-CNTs and t-CNTs were listed in Table 2. The oxygen content was increased from 5.25% to 9.72% and the ratio of oxygen to carbon (O/C) of CNTs was increased from 5.57% to 10.83% after acid treatment, indicating that the acid treatment introduced the oxygen functional groups on the surface of CNTs.

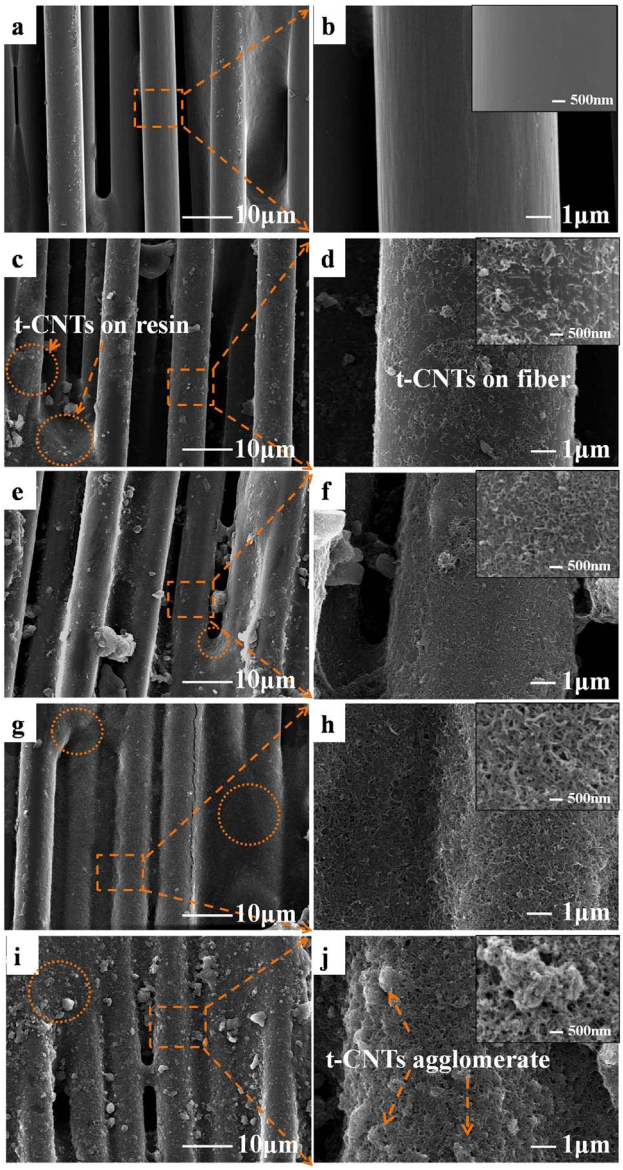

Fig. 4. SEM images of CF/PEEK prepregs with different t-CNTs content: (a, b) 0, (c, d) 0.1 wt%, (e, f) 0.3 wt%, (g, h) 0.5 wt% and (i, j) 1.0 wt%. (The inset was SEM images with higher magnification). (For interpretation of the references to color in this figure legend, the reader is referred to the web version of this article.)

As shown in Fig. 2, the spectra of C1s could be fitted into five peaks, including graphitic C (284.60 eV), phenolic or ether alcohol group (286.10–286.30 eV), carbonyl group (287.30–287.60 eV), ester or carboxyl group (288.40–288.90 eV) and π–π* (290.40–290.80 eV) [23]. The binding energies (BE) and percent contribution (PC) of various functional groups were listed in Table 3. It could be apparently found

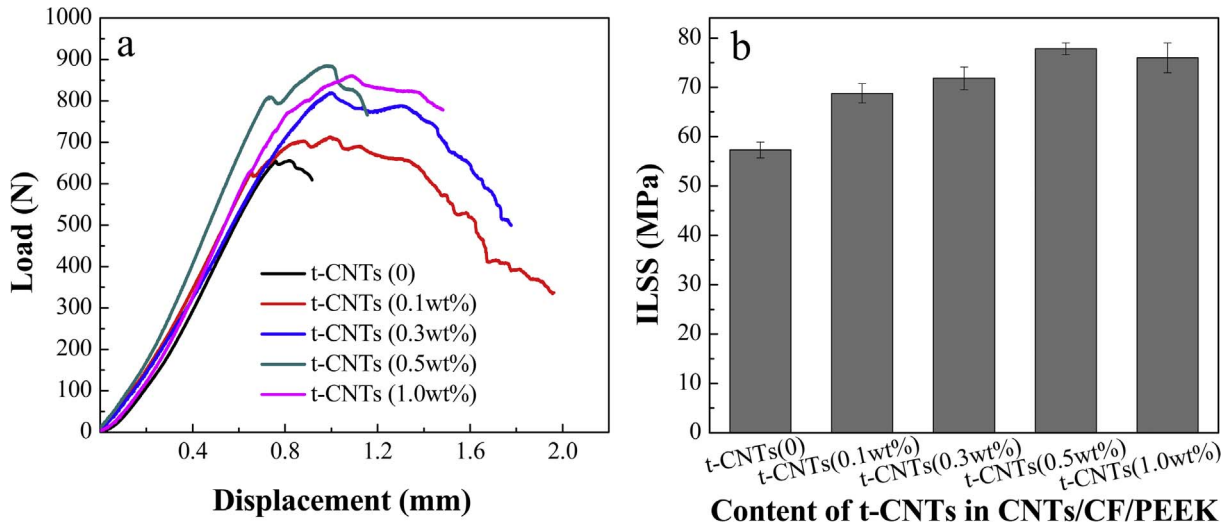

Fig. 5. The ILSS of CNTs/CF/PEEK composites with different t-CNTs content: (a) Typical load-displacement curve and (b) interlaminar shear strength of composites. (For interpretation of the references to color in this figure legend, the reader is referred to the web version of this article.)

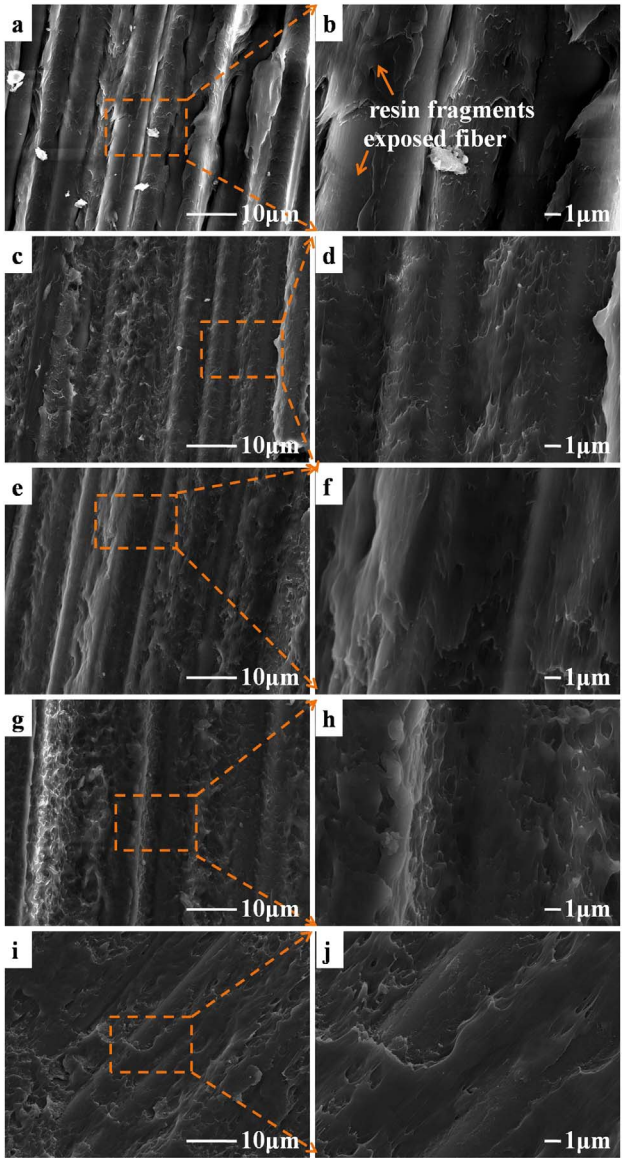

Fig. 6. SEM images of ILSS failure surface of CNTs/CF/PEEK composites with different t-CNT content: (a, b) 0, (c, d) 0.1 wt%, (e, f) 0.3 wt%, (g, h) 0.5 wt% and (i, j) 1.0 wt%. (For interpretation of the references to color in this figure legend, the reader is referred to the web version of this article.)

that the peaks of phenolic or ether alcohol group, carbonyl group and ester or carboxyl group were enhanced after the acid treatment, leading to the increment of the oxygen-containing functional groups from 24.34% to 33.64%. Therefore, the results of XPS demonstrated that the acid treatment assisted with ultrasonic was an effective way to enhance activated carbon atoms on CNTs surface.

Fig. 3 illustrated the digital photos of CNTs dispersion. It indicated that u-CNTs presented poor dispersion in water and it was easily accumulated within 1 min (Fig. 3a). After acid treatment, t-CNTs were well dispersed in water after 10 months (Fig. 3b), which was mainly ascribed to the electrostatic force of oxygen functional groups on its surfaces. The excellent dispersion of t-CNTs in water could maintain the uniform concentration during the whole spraying process.

3.2. The morphology of prepregs

The surface morphologies of prepregs without or with t-CNTs were shown in Fig. 4. As depicted in Fig. 4a and b, the surface of CF/PEEK prepregs was relatively neat and the resin was spread among CF. After spraying, the t-CNTs were evenly dispersed in CF surfaces, as well as in resin surfaces (marked in dashed circle), as shown in Fig. 4c–j. Heating in spraying process could well scatter the t-CNTs and prevented the formation of agglomerates probably for the rapid evaporation of water [24,25]. However, some agglomerates appeared when the t-CNTs content reached 1.0 wt%, as shown in Fig. 4i–j.

Energy dispersive spectroscopy (EDS) was performed to determine the atomic content of C, N and O, as well as the dispersion state of t-CNTs on CF. The atomic content and the EDS mapping were listed in Table S1 and Fig. S1, respectively. After acid treatment, the surface oxygen content of CNTs was increased by the result of XPS. Thus, the increased oxygen content on the surface of CF after spraying can be attributed to the incorporating of t-CNTs. As present in Table S1, the surface oxygen content of CF was increased with t-CNTs content increment. Also, the uniform increased oxygen on CF suggested the uniform distribution of t-CNTs on the surface of CF (Fig. S1).

3.3. Interlaminar shear strength of composites

The SBS test is an effective technique to evaluate the ILSS, which can reflect the combination of fiber and resin [26]. The typical load-displacement curves of CNTs/CF/PEEK composites were presented in Fig. 5a. The maximum load during SBS test was needed after incorporating t-CNTs, illustrating t-CNTs could improve the ILSS of composite. As shown in Fig. 5b, the ILSS of CF/PEEK was 57.3 MPa,

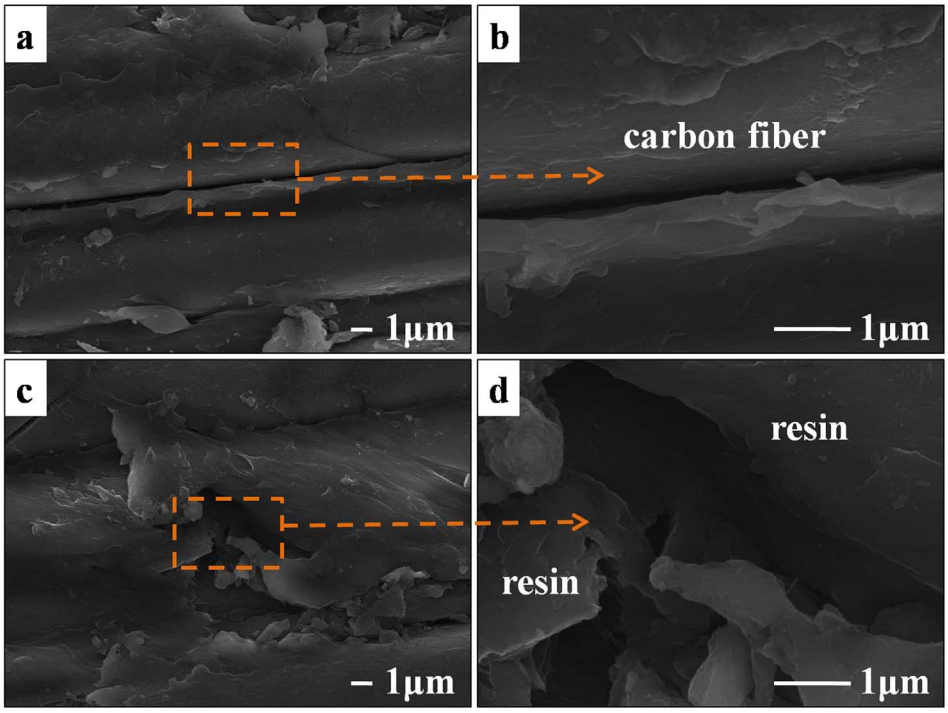

Fig. 7. SEM images of crack propagation region of CF/PEEK: (a, b) interface region and (c, d) resin region. (For interpretation of the references to color in this figure legend, the reader is referred to the web version of this article.)

while it reached to 68.8 MPa, 71.8 MPa, 77.8 MPa and 76.0 MPa when 0.1 wt%, 0.3 wt%, 0.5 wt% and 1.0 wt% t-CNTs were introduced into CF/PEEK composites. The ILSS of composites with 1.0 wt% t-CNTs slightly decreased compared with that of the composites with 0.5 wt% t-CNTs, because high t-CNTs content was unfavorable for the impregnation of CF by resin and the existence of t-CNTs aggregates (Fig. 4i and j) also produced stress concentration region [14].

It is well known that CNTs could be incorporate into fiber reinforced polymer composites (FRPs) by various methods, such as dispersing CNTs in matrix, growing or grafting on the fibers surface and inserting CNTs buckypaper into laminar interface. The PEI/MWCNT/CF composites were prepared by firstly dispersing CNTs in PI film. The ILSS of these composites were decreased after adding MWCNT compared to their reference specimen due to CNT agglomerate effect in resin [27]. It was worth to mention that the improvement of ILSS of 21.6% and 31.6% were obtained for the CF-CNTs composites and CF-CNTs-POSS composites using grafting, respectively, compared with desized carbon fiber reinforced composites [28]. However, the preparation of multiscale thermoplastics composites is scarce in documents, especially for high-performance thermoplastic composites. In here, the ILSS of composites was increased by 35.8% after incorporating 0.5 wt% t-CNTs by prepreg spraying method, which was a facile approach for preparation of the multiscale composites. Moreover, it avoids the viscosity increase in high thermoplastic composites. Some comparison in mechanical properties of FRPs was listed in Table S2 [7,10,27–29].

For CFRPs, the interlaminar shear failure involves several modes, such as adhesive failure, mixed failure and cohesive failure [30]. Poor fiber-resin interfacial adhesion will result in adhesive failure or mixed failure, whereas strong interfacial adhesion is beneficial to stress transfer and make the cohesive failure becomes the dominate mode. The SEM images of composites failure surface after SBS test were displayed in Fig. 6. For CF/PEEK composites, part of fibers was exposed and there were fewer resin fragments remain on CF surface (Fig. 6a and b), illustrating the poor fiber-resin interfacial adhesion. The poor interfacial adhesion restrained the load transfer between fiber and resin, leading to the crack initiation and propagation in interface and lowering the ILSS. Compared with CF/PEEK composites, some resin fragments were remained on CF surface after incorporating t-CNTs into composites (Fig. 6c-6j), indicating the good fiber-resin interfacial adhesion of CNTs/CF/PEEK composites.

To better understand the effect of incorporated t-CNTs on the interfacial adhesion of CNTs/CF/PEEK composites, the crack propagation region of composites without and with t-CNTs was depicted in Figs. 7 and 8, respectively. For CF/PEEK composites, the fracture region was smooth (Fig. 7a and b). After incorporating 0.5 wt% t-CNTs, there was still partial connection between CF and resin after failure for CNTs/CF/PEEK (Fig. 8a and b). And the presence of t-CNTs (Fig. 8c and d) could be observed at the fracture surface, extending into resin region. The images provided direct evidence of interlocking.

Besides the interfacial adhesion, the fracture of CFRPs is also determined by resin [31]. For CF/PEEK composites, the resin showed less deformation (Fig. 7c and d), suggesting the poor resistance to crack propagation. However, for composites with 0.5 wt% t-CNTs, the addition of t-CNTs improved the ductility of resin, making the fracture surface become rougher and the resin show larger deformation (Fig. 8e and f). And t-CNTs could hinder the crack growing by bridge effect, which could release of stress and absorb higher energy [13,32]. Meanwhile, the diameter of pulled-out t-CNTs was longer than the raw one indicating good wetting of t-CNTs by resin. Moreover, the t-CNTs pulling out (Fig. 8g and h) instead of t-CNTs breaking was also contributed to the improvement of ILSS due to the energy dissipation by pulling force of t-CNTs [33]. Such deflections illustrated that the t-CNTs with high elastic modulus in resin region could improve the ductile properties of resin and restrain the propagation of crack by bridge effect, which absorbed energy and improved ILSS as Scheme 3.

3.4. Flexural properties of composites

The 0° flexural strength and flexural modulus were measured to evaluate the bending resistance of composites. The typical load-displacement curves of CNTs/CF/PEEK composites were shown in Fig. 9a. The maximum load in flexural test was increased after introducing t-CNTs in composites, and bending resistance was improved. As shown in Fig. 9b, the flexural strength and flexural modulus of CF/PEEK were

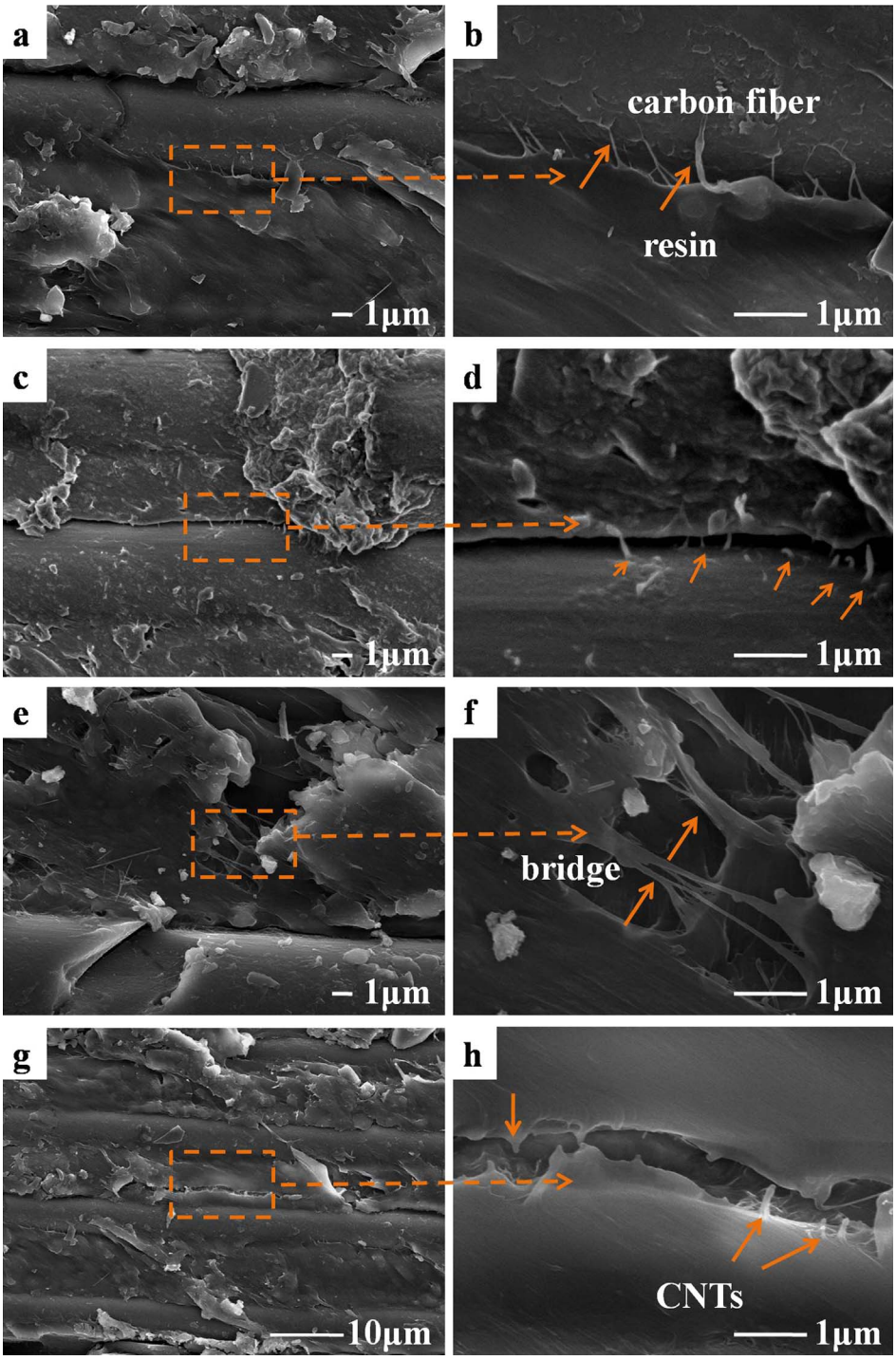

Fig. 8. SEM images of crack propagation region of CNTs (0.5 wt%)/CF/PEEK: (a–d) interface region and (e–h) resin region. (For interpretation of the references to color in this figure legend, the reader is referred to the web version of this article.)

1226.0 MPa and 64.5 GPa, respectively. After spraying t-CNTs with the content of 0.1 wt%, 0.3 wt%, 0.5 wt% and 1.0 wt%, the flexural strength of composites increased to 1308.3 MPa, 1457.7 MPa, 1537.3 MPa and 1316.2 MPa, respectively; and flexural modulus of composites increased to 65.3 GPa, 65.6 GPa, 79.8 GPa and 70.7 GPa, respectively. The flexural strength and flexural modulus of composite with 1.0 wt% t-CNTs were slightly decreased compared with those of composite with 0.5 wt% t-CNTs due to CNTs aggregation.

In present work, the flexural strength and flexural modulus of CNTs/CF/PEEK composites were increased by 25.4% and 23.7% after incorporating 0.5 wt% t-CNTs by prepreg spraying method. An increment of 11.6% and 18.0 wt% on flexural strength and modulus was obtained for CNT/CF/epoxy composites by mixing CNT in resin after 10 min ultrasonic; and 8.6% and 8.4% on flexural strength and modulus was obtained after 3 h ultrasonic [10]. The CNT might well disperse in resin by prolonging ultrasonic, but it also led to the increment of resin viscosity which was detrimental to the infusion process. In this work, the significant improvement in flexural properties was related to the good ductility of resin. According to the results of ILSS, the addition of t-CNTs could improve the ductility of resin, which wasted a lot of energy and elevated the flexural properties [34]. Meanwhile, the flexural properties of composites were also determined by the fiber-

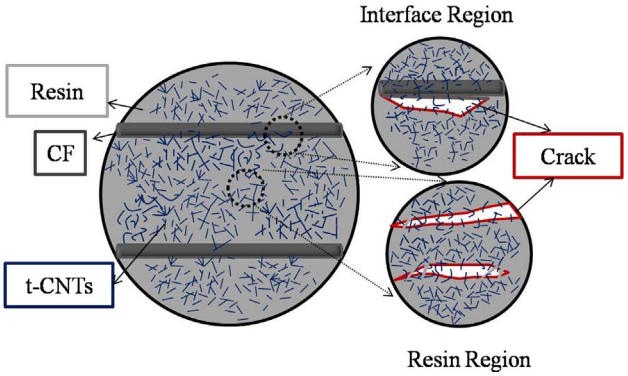

Scheme 3. Schematic of reinforcement. (For interpretation of the references to color in this figure legend, the reader is referred to the web version of this article.)

resin interfacial adhesion. As shown in Fig. 10, few resin fragments were remained on the surface of CF after flexural failure for the CF/PEEK composites, whereas the amount of resin fragments was increased on the surface of CF with the addition of t-CNTs due to the strong fiber-resin adhesion.

3.5. Electrical conductivity

The low electrical conductivity of CFRPs limited their widely application in aerospace industries and electronics field, when they were used as lightning strike protection materials, electromagnetic shielding materials, etc. It is well known that CNTs in composites could act as conductive fillers to improve the electrical conductivity [35–37]. The anisotropic behavior of electrical conductivity has been verified in many CFRPs. Therefore, 0° and through-thickness electrical conductivity were calculated at room temperature to evaluate the influence of the t-CNTs on the electrical conductivity of the composites.

The 0° electrical conductivity of CF/PEEK was 0.39 S/cm, indicating that CF play a conductivity role in composites, as the pure PEEK was an insulating polymer ($\sigma < 10^{-13}$ S/cm) [34] . As shown in Fig. 11a, the 0° electrical conductivity of t-CNTS/CF/PEEK composites was increased by 131% after incorporating 1.0 wt% t-CNTs, compared with CF/PEEK composites. Such a markedly enhancement of 176% was reported by adding 4.95 wt% CNT backypapers (BP) in CF/epoxy prepreg compared with neat CF/epoxy composites. The enhancement of electrical conductivity in references resulted from the superior electrical conductivity of CNT network formed by BP, which were measured as approximately 855 S/cm [38]. In this work, t-CNTs were evenly sprayed in prepreg

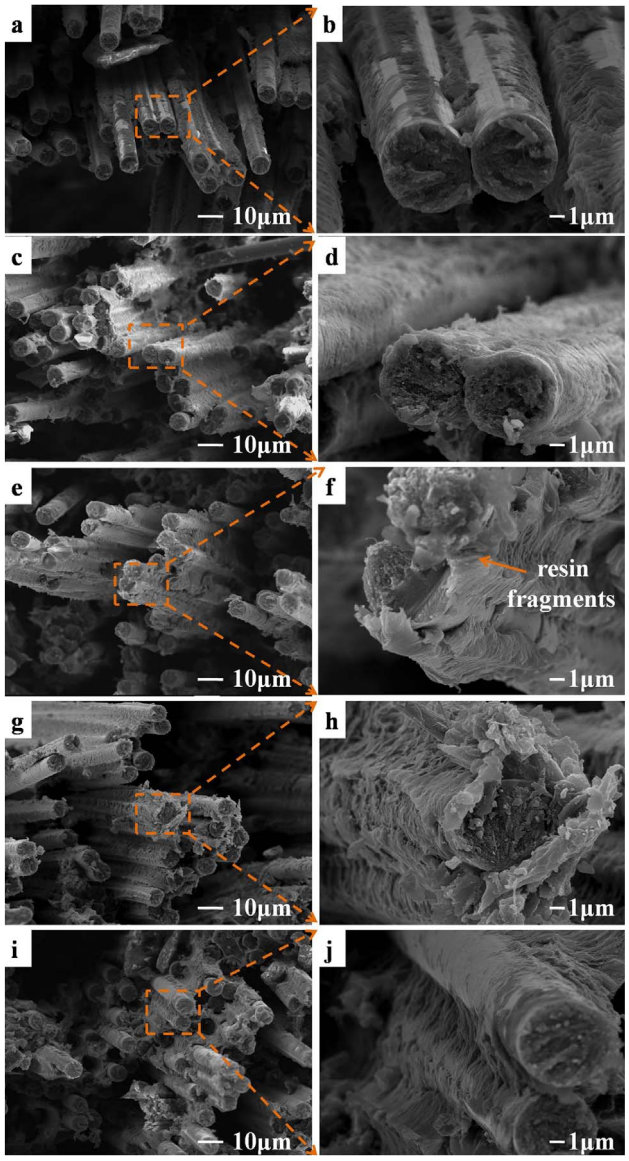

Fig. 10. SEM images of flexural failure surface of CNTs/CF/PEEK composites with different t-CNTs content: (a, b) 0, (c, d) 0.1 wt%, (e, f) 0.3 wt%, (g, h) 0.5 wt% and (i, j) 1.0 wt%. (For interpretation of the references to color in this figure legend, the reader is referred to the web version of this article.)

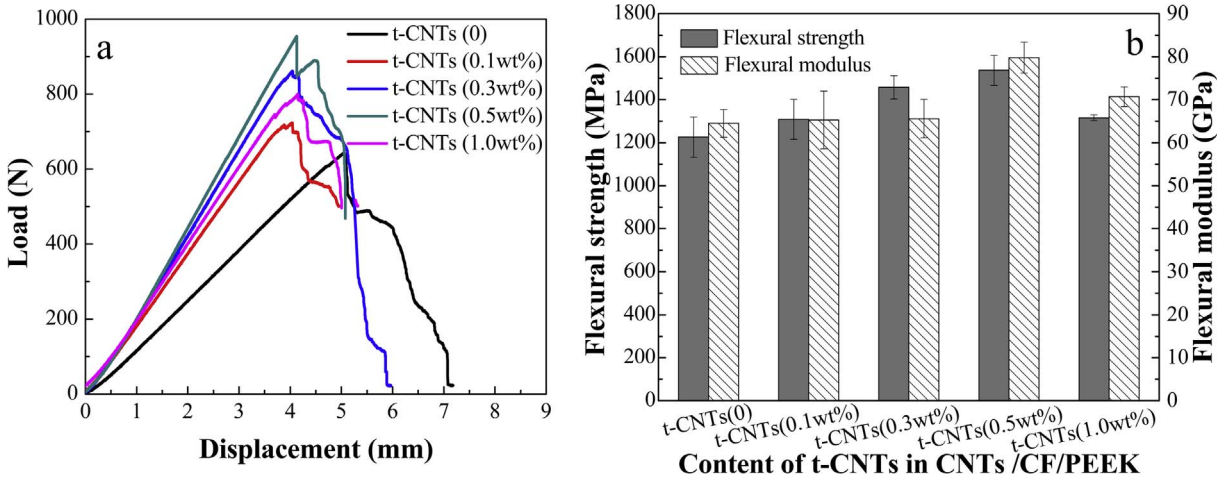

Fig. 9. The flexural properties of CNTs/CF/PEEK composites with different t-CNTs content: (a) Typical load-displacement curve and (b) flexural strength and flexural modulus of composites. (For interpretation of the references to color in this figure legend, the reader is referred to the web version of this article.)

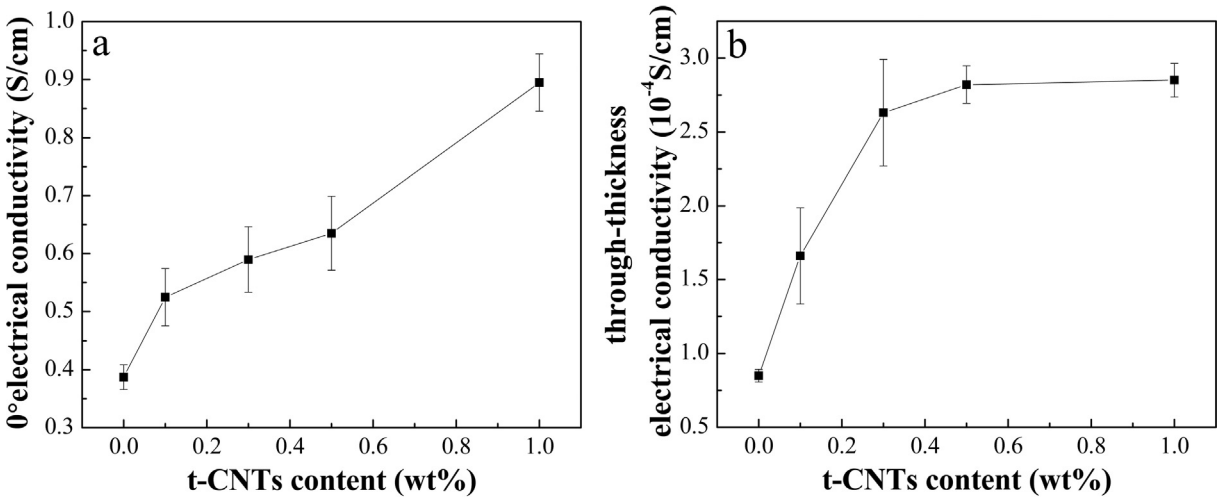

Fig. 11. The electrical conductivity of CNTs/CF/PEEK composites: (a) 0° direction and (b) through thickness direction.

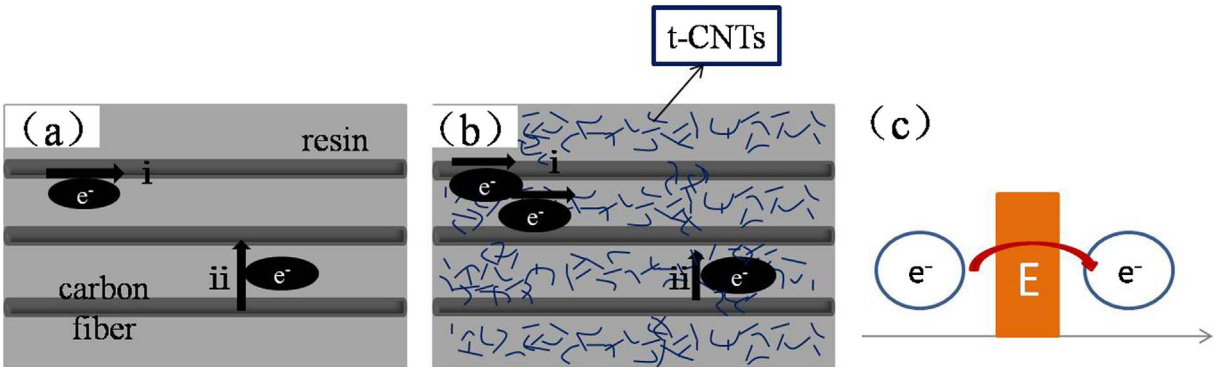

Scheme 4. The schematic of electrical transporting: (a) composites without t-CNTs; (b) composites with t-CNTs; (c) tunnel effect (E represents the barriers during electron transporting). (i:electron transport along 0° direction; ii: electron transport along through-thickness direction). (For interpretation of the references to color in this figure legend, the reader is referred to the web version of this article.)

Table 4
Through-thickness thermal conductivity results of composites.

	t-CNTs (0)	t-CNTs (0.1 wt%)	t-CNTs (0.3 wt%)	t-CNTs (0.5 wt%)	t-CNTs (1.0 wt%)
Through-thickness thermal conductivity (W/(m·K))	0.97	1.06	1.07	1.14	1.15
Increase (%)	0	9.3	10.3	17.5	18.6

(Fig. 4) and showed the similar structure as BP in references. Among them, the t-CNTs could form an effective conductive pathway in resin rich region between two prepreg plies, facilitating the electron "pass-through" the composites.

The through-thickness electrical conductivity (Fig. 11b) of CF/PEEK composites was quite low (0.85×10^{-4} S/cm), which was mainly attributed to the long distances between adjacent fibers of CF/PEEK composites, and electron was difficult to transport. After the addition of t-CNTs, the existence of t-CNTs network in resin rich region could connect adjacent fibers and it was benefit to the electron transport, thus increased the through-thickness electrical conductivity of composites. Moreover, some isolated t-CNTs could also promote electron transporting through "tunneling effect" under the electronic filed [39]. The schematic of electrical transporting was illustrated in Scheme 4.

It could be seen that the electrical conductivity of composite was several orders of magnitude less than that of the pure CNTs because the electron transferring in composites was restrained by the interfacial electrical resistance between t-CNTs and resin as well as t-CNTs itself.

3.6. Thermal conductivity

Due to the thermal conductivity of CFRPs is an important property for many applications, CNTs with high thermal conductivity can be used as nanofillers to improve the thermal conductivity of composites. The through-thickness thermal conductivities of CNTs/CF/PEEK composites with different t-CNTs content were listed in Table 4. The thermal conductivity of the CF/PEEK composites was 0.97 W/(m·K), while the introduction of t-CNTs to composites could increase the thermal conductivity as the formation of effective thermal conductive pathway, which will connect adjacent CF and increase the chance for phonons transporting in through-thickness direction [34].

It could be seen that the improvement of thermal conductivity was lower than our expectation, probably related to the fact that the thermal transferring was restrained by the interfacial thermal resistance between t-CNTs and resin as well as t-CNTs itself [40]. As a result, the quantity for forming the effective phonon transporting network was less than t-CNTs content.

4. Conclusion

In this work, CNTs/CF/PEEK multiscale composites with different t-CNTs content were prepared by prepreg spraying method. The obtained composites showed excellent mechanical properties. Compared with CF/PEEK, the ILSS of CNTs/CF/PEEK composite with 0.5 wt% t-CNTs was increased by 35.8% from 57.3 MPa to 77.8 MPa. Meanwhile, the flexural strength and flexural modulus of composites with 0.5 wt% t-CNTs was increased by 25.4% and 23.7%, respectively. This enhancement of the mechanical properties was mainly attributed to the mechanical interlocking effect of t-CNTs, which improved the combination of fiber and matrix. Furthermore, the addition of t-CNTs in resin region acted as bridge to restrain the crack propagation. Moreover, the addition of t-CNTs could improve the electrical conductivity and thermal conductivity of composites by forming an effective conductive pathway. Therefore, spraying the t-CNTs dispersions on the CF/PEEK prepregs is a facile method to effectively improve the mechanical, electrical and thermal properties of composites.

Acknowledgement

This work was supported by Natural Science Foundation of Shanxi Province (Grant numbers 2015011032), National Natural Science Foundation of China (Grant numbers U1510119), Innovation Foundation of China (Grant numbers CXJJ-16M127), and Youth Innovation Promotion Association Funds for Chinese Academy of Science (Grant numbers 2012140).

Appendix A. Supplementary material

Supplementary data associated with this article can be found, in the online version, at http://dx.doi.org/10.1016/j.compositesa.2018.02.030.

References

[1] Soutis C. Carbon fiber reinforced plastics in aircraft construction. Mater Sci Eng A 2005;412(1):171–6.
[2] Mitschang P, Blinzler M, Wöginger A. Processing technologies for continuous fibre reinforced thermoplastics with novel polymer blends. Compos Sci Technol 2003;63(14):2099–110.
[3] Mouritz AP, Gellert E, Burchill P, Challis K. Review of advanced composites structures for naval ships and submarines. Compos Struct 2001;53(1):21–41.
[4] Dong Q, Guo YL, Chen JL, Yao XL, et al. Influencing factor analysis based on electrical–thermal-pyrolytic simulation of carbon fiber composites lightning damage. Compos Struct 2016;140:1–10.
[5] Wen J, Xia ZH, Choy F. Damage detection of carbon fiber reinforced polymer composites via electrical resistance measurement. Composites Part B 2011;42(1):77–86.
[6] Peng QY, He XD, Li YB, Wang C, et al. Chemically and uniformly grafting carbon nanotubes onto carbon fibers by poly(amidoamine) for enhancing interfacial strength in carbon fiber composites. J Mater Chem 2012;22(13):5928–31.
[7] Deng C, Jiang JJ, Liu F, Fang LC, et al. Influence of carbon nanotubes coatings onto carbon fiber by oxidative treatments combined with electrophoretic deposition on interfacial properties of carbon fiber composite. Appl Surf Sci 2015;357:1274–80.
[8] Bekyarova E, Thostenson ET, Yu A, Kim H, et al. Multiscale carbon nanotube-carbon fiber reinforcement for advanced epoxy composites. Langmuir 2007;23(7):3970–4.
[9] Díez-Pascual AM, Naffakh M. Tuning the properties of carbon fiber-reinforced poly (phenylene sulphide) laminates via incorporation of inorganic nanoparticles. Polymer 2012;53(12):2369–78.
[10] Kim MS, Park YB, Okoli OI, Zhang C. Processing, characterization, and modeling of carbon nanotube-reinforced multiscale composites. Compos Sci Technol 2009;69(3–4):335–42.
[11] Díez-Pascual AM, Guan JW, Simard B, Gómez-Fatou MA. Poly (phenylene sulphide) and poly (ether ether ketone) composites reinforced with single-walled carbon nanotube buckypaper: II – Mechanical properties, electrical and thermal conductivity. Composites Part A 2012;43(6):1007–15.
[12] Song L, Zhang H, Zhang Z, Xie SS. Processing and performance improvements of SWNT paper reinforced PEEK nanocomposites. Composites Part A 2007;38(2):388–92.
[13] Ashrafi B, Díez-Pascual AM, Johnson L, Genest M, et al. Processing and properties of PEEK/glass fiber laminates: effect of addition of single-walled carbon nanotubes. Composites Part A 2012;43(8):1267–79.
[14] Shen ZQ, Bateman S, Wu DY, McMahon P, et al. The effects of carbon nanotubes on mechanical and thermal properties of woven glass fibre reinforced polyamide-6 nanocomposites. Compos Sci Technol 2009;69(2):239–44.
[15] Shazed MA, Suraya AR, Rahmanian S, Mohd Salleh MA, et al. Effect of fibre coating and geometry on the tensile properties of hybrid carbon nanotube coated carbon fibre reinforced composite. Mater Des 2014;54(2):660–9.
[16] Zhao F, Huang YD, Liu L, Bai YP, et al. Formation of a carbon fiber/polyhedral oligomeric silsesquioxane/carbon nanotube hybrid reinforcement and its effect on the interfacial properties of carbon fiber/epoxy composites. Carbon 2011;49(8):2624–32.
[17] Gao SL, Kim JK. Cooling rate influences in carbon fibre/PEEK composites. Part 1. Crystallinity and interface adhesion. Composites Part B 2000;31(6):517–30.
[18] Nguyen HX, Ishida H. Poly(ary1-ether-ether-ketone) and its advanced composites: a review. Polym Compos 1987;8(2):57–73.
[19] Patel P, Hull TR, Lyon RE, Stoliarov SI, et al. Investigation of the thermal decomposition and flammability of PEEK and its carbon and glass-fibre composites. Polym Degrad Stab 2011;96(1):12–22.
[20] Sharma M, Bijwe J, Mitschang P. Wear performance of PEEK–carbon fabric composites with strengthened fiber–matrix interface. Wear 2011;271(9–10):2261–8.
[21] Davies P, Riou L, Mazeas F, Warnier P. Thermoplastic composite cylinders for underwater applications. J Thermoplast Compos Mater 2005;18(5):417–43.
[22] Bismarck A, Hofmeier M, Dörner G. Effect of hot water immersion on the performance of carbon reinforced unidirectional poly(ether ether ketone) (PEEK) composites: stress rupture under end-loaded bending. Composites Part A 2007;38(2):407–26.
[23] Ma PC, Kim JK, Tang BZ. Functionalization of carbon nanotubes using a silane coupling agent. Carbon 2006;44(15):3232–8.
[24] Kaempgen M, Duesberg GS, Roth S. Transparent carbon nanotube coatings. Appl Surf Sci 2005;252(2):425–9.
[25] Bu Q, Zhan YH, He FF, Lavorgna M, et al. Stretchable conductive films based on carbon nanomaterials prepared by spray coating. J Appl Polym Sci 2015;113(15):43243–50.
[26] Teuber L, Fischer H, Graupner N. Single fibre pull-out test versus short beam shear test: comparing different methods to assess the interfacial shear strength. J Mater Sci 2013;48(8):3248–53.
[27] Lu YH, Zhan MS, Zheng WH. Preparation and properties of T300 carbon fiber reinforced thermoplastic polyimide composites. J Appl Polym Sci 2006;102(1):646–54.
[28] Zhang RL, Wang CG, Liu L, Cui HZ, et al. Polyhedral oligomeric silsesquioxanes/carbon nanotube/carbon fiber multiscale composite: influence of a novel hierarchical reinforcement on the interfacial properties. Appl Surf Sci 2015;353:224–31.
[29] Veedu VP, Cao AY, Li XS, Ghasemi-Nejhad MN, et al. Multifunctional composites using reinforced laminae with carbon-nanotube forests. Nat Mater 2006;5(6):457–62.
[30] Liu Z, Tang C, Chen P, Yu Q, et al. Modification of carbon fiber by air plasma and its adhesion with BMI resin. RSC Adv 2014;4(51):26881–7.
[31] Khan SU, Kim JK. Improved interlaminar shear properties of multiscale carbon fiber composites with Bucky paper interleaves made from carbon nanofibers. Carbon 2012;50(14):5265–77.
[32] Liu TX, Phang IY, Shen L, Chow SY, et al. Morphology and mechanical properties of multiwalled carbon nanotubes reinforced nylon-6 composites. Macromolecules 2004;37(19):7214–22.
[33] Díez-Pascual AM, Naffakh M, Marco C, Gómez-Fatou MA, et al. Multiscale fiber-reinforced thermoplastic composites incorporating carbon nanotubes: a review. Curr Opin Solid State Mater Sci 2014;18(2):62–80.
[34] Díez-Pascual AM, Ashrafi B, Naffakh M, González-Domínguez JM. Influence of carbon nanotubes on the thermal, electrical and mechanical properties of poly (ether ether ketone)/glass fiber laminates. Carbon 2011;49(8):2817–33.
[35] Zhang R, Dowden A, Deng H, Baxendale M, et al. Conductive network formation in the melt of carbon nanotube/thermoplastic polyurethane composite. Compos Sci Technol 2009;69(10):1499–504.
[36] Wichmann MHG, Sumfleth J, Gojny FH, Quaresimin M, et al. Glass-fibre-reinforced composites with enhanced mechanical and electrical properties – benefits and limitations of a nanoparticle modified matrix. Eng Fract Mech 2006;73(16):2346–59.
[37] Moisala A, Li Q, Kinloch IA, Windle AH. Thermal and electrical conductivity of single- and multi- walled carbon nanotube-epoxy composites. Compos Sci Technol 2006;66(10):1285–8.
[38] Wang SK, Downes R, Young C, Haldane D, et al. Carbon fiber/carbon nanotube buckypaper tnterply hybrid composites: manufacturing process and tensile properties. Adv Eng Mater 2015;17(10):1442–53.
[39] Nieves CA, Ramos I, Pinto NJ, Zimbovskaya NA. Electron transport mechanisms in polymer-carbon sphere composites. J Appl Phys 2016;120(1):675–82.
[40] Shin YC, Novin E, Kim HS. Electrical and thermal conductivities of carbon fiber composites with high concentrations of carbon nanotubes. Int J Precis Eng Man 2015;16(3):465–70.